A nonlinear energy harvester for torsional oscillations

B. E. Gunn, S. Theodossiades, S. J. Rothberg
Loughborough University, Wolfson School of Mechanical, Electrical and Manufacturing Engineering
Loughborough, Leicestershire, LE11 3TU
e-mail: **S.Theodossiades@lboro.ac.uk**

Abstract
Torsional fluctuations around the mean speed of a rotating shaft represent a typical source of undesirable energy losses in many industrial applications. Furthermore, many control and structural health monitoring systems in rotordynamics require an ever-increasing number of sensors. Currently, powering a wireless sensor mounted on a rotating shaft is feasible using either slip rings or batteries, both of which often incur high maintenance costs in applications with difficult access or when idle due to malfunction. In this paper, an electromagnetic energy harvester prototype is manufactured by adapting a commercially available permanent magnet DC motor. The energy harvesting capabilities of the device are preliminary tested and compared to theoretical predictions.

1 Introduction

Vibration energy harvesters are becoming increasingly widespread as a means of powering small, low power electronic wireless sensors for control and system health monitoring systems. Due to the often unavoidable, undesirable and ubiquitous nature of vibrations in engineering applications, vibration energy harvesters can provide a virtually endless supply of energy for such sensors without the need for regular maintenance or complicated wiring harnesses. This is ideal for applications where servicing such a system could be tedious or cause severe costs due to machine down time.

One such environment is that of rotating shafts which exhibit torsional speed fluctuations. Such rotordynamics are hard to avoid in industrial applications; however, often these speed fluctuations are undesirable and can lead to durability issues if not suitably addressed. Typically, these vibrations are absorbed by mechanical vibration dampers which ultimately dissipate this energy as heat, representing an energy loss from the system.

Past research involving energy harvesters in rotordynamics include Kim [1] and Trimble et al [2]. Kim implemented a piezoelectric cantilever beam which protruded radially from a rotating shaft connected to an internal combustion engine. The aim was to harness energy excess from the second order speed fluctuations of the shaft. Due to centripetal acceleration effects, the beam stiffens as the shaft speed increases, which allowed the harvester to remain at resonance throughout the operating speed range of the engine. However, it was concluded that little power could be scavenged from this device.

Trimble et al [2] used an electromagnetic energy harvester to extract torsional vibration energy from an oil well drill to power a wireless sensor. Their device was capable of harvesting 205mW at resonance and 74 mW when excited using real world random vibrations measured from the drill. However, by using an energy harvester that operates away from resonance, a larger proof mass is needed compared to when the energy harvester is resonating. In the present work, where the shaft has a clear second order speed fluctuation about its mean speed ranging from around 800 rpm to 4000 rpm, such an approach is not ideal; hence some method of maintaining resonance is sought.

Other researchers have investigated harvesters which extract energy from the mean speed of rotating components for applications, such as automotive tyre pressure monitoring systems. Roundy et al [3] used a self-tuning pendulum arrangement to ensure their device was at resonance at any tyre speed. It employed a

frequency up converting mechanism to pluck piezoelectric beams that were able to resonate. Such a device has benefits at low speeds where the piezoelectric components cause bistable response whereas at high speeds the centripetal acceleration dominates and allows the harvester to resonate at speed.

Gu and Livermore [4], [5] developed self-tuning energy harvesters which were tuned using the centripetal acceleration to resonate at a wide speed range. Meanwhile, other researchers such as Mann and Sims [6] and Liu and Yuan [7] have employed a cubic nonlinear stiffness to increase the operating frequency range of their axial harvesters.

To the authors' knowledge, the present work is the first cubic nonlinear energy harvester application for torsional shaft speed fluctuations. An electromagnetic energy harvester is used to generate electricity from torsional oscillations. The device uses a cubic nonlinear spring and has, in a previous work, shown potential to work across the full operating range of the shaft. In this paper, preliminary experimental results of a tested physical prototype are presented. An introduction to the experimental set up is followed by a description of the physical device. A typical frequency response function follows. Then, the experimental results are presented and the main conclusions are drawn.

2 Nomenclature

A	Dimensionless constant of acceleration
c_{mech}	Mechanical damping coefficient
I	Electric current
J	Mass moment of inertia
k_1	Linear coefficient of stiffness
k_3	Cubic coefficient of stiffness
t	Time
$\dot{\alpha}_1$	Angular velocity of the driving shaft
$\dot{\alpha}_2$	Angular velocity of the driven shaft
$\dot{\beta}$	Angular velocity of the energy harvester rotor
γ	Angle between driving and driven shaft
$\hat{\theta}$	Electromagnetic coupling factor

3 Description of the device

In this section, the experimental test rig is presented followed by a brief description of the energy harvester itself. The key characteristics of a typical nonlinear energy harvester are then discussed.

3.1 Excitation environment

To emulate the torsional speed fluctuations often present in rotordynamics, the energy harvester is mounted on the end of an unloaded shaft. The latter is driven by an electric motor through a universal joint that is

intentionally set at an angle in order to induce second order speed fluctuations from which the energy harvester will extract its power. Figure 1 shows a schematic depiction of the test rig.

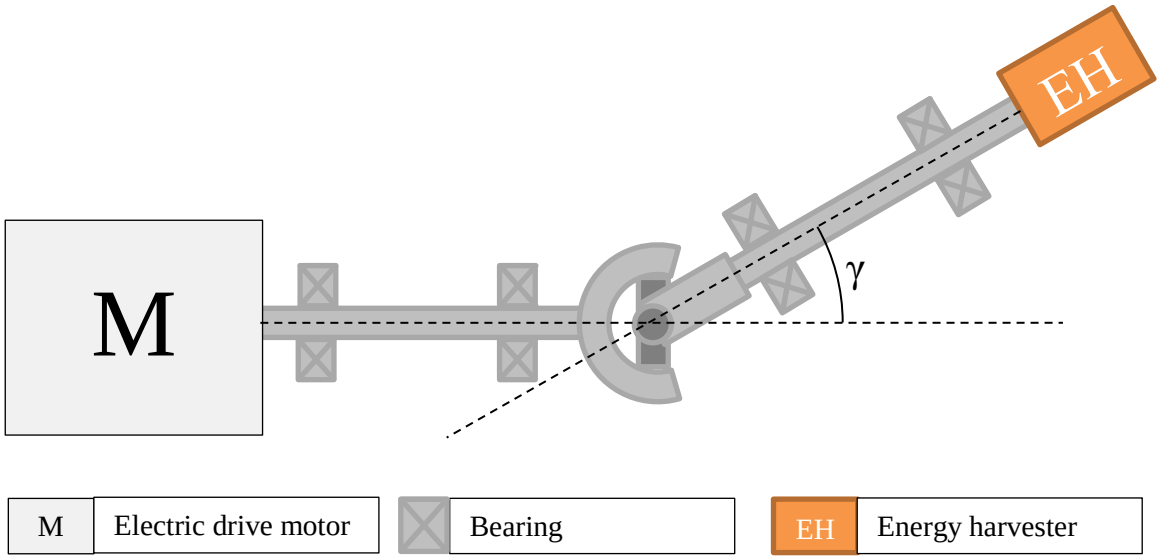

Figure 1: Schematic diagram of the energy harvester test rig

The angular velocity of the driven shaft, α_2, is calculated using the angular velocity of the driving shaft, α_1, using Eqn. (1) [8]:

$$\dot{\alpha}_2 = \frac{\dot{\alpha}_1 cos\gamma}{1 - \sin^2\gamma\cos^2\alpha_1} \tag{1}$$

Differentiating Eqn. (1) with respect to time yields the acceleration of the driven shaft:

$$\ddot{\alpha}_2 = \frac{\ddot{\alpha}_1 cos\gamma}{1 - \sin^2\gamma\cos^2\alpha_1} - \frac{\dot{\alpha}_1^2 cos\gamma \sin^2\gamma\, sin2\alpha_1}{(1 - \sin^2\gamma\cos^2\alpha_1)^2} \tag{2}$$

Where γ denotes the angle between the rotating axes of the two shafts.

Assuming the inertia of the driving shaft is significantly larger than that of the driven shaft, the acceleration of the driving shaft will not be affected by the universal joint, thus the first term of Eqn. (2) can be neglected. The resulting acceleration with a constant drive speed is therefore approximated by

$$\ddot{\alpha}_2 = -A\dot{\alpha}_1^2 \sin(2\dot{\alpha}_1 t) \tag{3}$$

Where A is a dimensionless constant which depends on the angle of the universal joint, γ.

3.2 Energy harvester

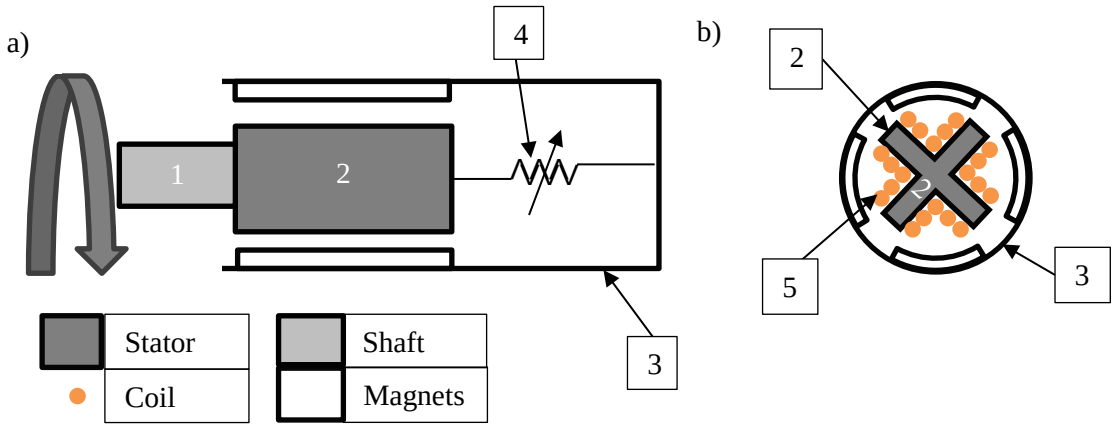

Figure 2: Schematic representation of the energy harvester: a) Side view and b) End view

An off-the-shelf external rotor brushless DC permanent magnet motor has been adapted to build the energy harvester. With reference to Figure 2, the stator (2) is made of a laminated iron core with series wound copper windings (5). The stator is mounted to the rotating shaft (1) and rotates with it. The rotor (3) comprises a housing with radially magnetized permanent magnets fixed to its inner surface. The rotor (3) is free to rotate around the stator (1) except for the cubic nonlinear torsional spring (4) whose torque is calculated as a function of the angular displacement:

$$T = k_1(\alpha_2 - \beta) + k_3(\alpha_2 - \beta)^3 \tag{4}$$

This nonlinear spring setting restricts the rotation of the rotor and allows for the rotor to oscillate torsionally with respect to the stator. When the rotor moves relative to the stator, the relative velocity induces an electromotive force in the coils which can power a load. In the present work, the electrical power is simply dissipated through a resistor with resistance matching the internal resistance of the coil. This introduces a damping effect on the mechanical system. The motion of the energy harvester is given by:

$$J\ddot{\beta} = k_1(\alpha_2 - \beta) + k_3(\alpha_2 - \beta)^3 + c_{mech}(\dot{\alpha}_2 - \dot{\beta}) + \hat{\theta}I \tag{5}$$

Where J denotes the mass moment of inertia of the rotor; β denotes the angular position of the rotor; α_2 is the angular position of the stator. An over dot denotes differentiation with respect to time. The linear component of the stiffness is denoted by k_1 and the cubic nonlinear stiffness coefficient is denoted by k_3. c_{mech} is the linear mechanical damping coefficient of the system and $\hat{\theta}I$ represents the power extracted by the electrical circuit with $\hat{\theta}$ being the nonlinear electromechanical coupling factor and I, the electric current in the load circuit.

A derivation of $\hat{\theta}$ can be found in Gunn et al [9], which is based on the work of Markovic and Perriard [10]. However, due to a malfunction in the physical prototype, the electrical load was disconnected during the tests, thus the $\hat{\theta}I$ term plays no role in the following experiments. The aim of this work is therefore to assess the dynamics of the system and its potential to generate power, neglecting any electrical effects.

3.3 Numerical model results

The AUTO 07p bifurcation analysis software [11] was used to perform numerical continuation of the energy harvester equation of motion (Eqn. (5)). Figure 3 shows a typical frequency response graph of the energy harvester. The response is similar to that of a Duffing oscillator; however, due to the frequency dependent amplitude of the excitation acceleration, there exists a condition where the jump down frequency is unattainable [9]. In the figure, the solid lines represent stable solutions and the dashed lines are unstable response that cannot be realised in a physical prototype. Below around 2800 rpm there is only one stable solution to the equations of motion. However, as the excitation frequency increases, the three-coinciding solutions region begins, where two responses are stable. The higher of the two stable solutions is the desired operating zone of the energy harvester, where naturally more power will be generated.

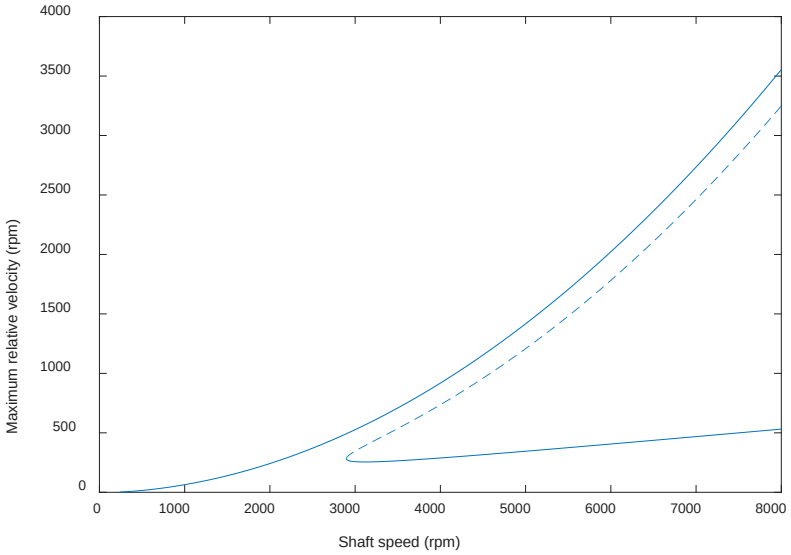

Figure 3: Typical frequency response graph of the energy harvester.

4 Experimental results

This section presents the results of tests conducted on a physical prototype. Typical time histories of the harvester's response are shown followed by the corresponding plot of the frequency response. The energy harvester behaves in a similar fashion to the numerical model presented in the previous section. Throughout this experiment, the universal joint is set at 20°, which induces sinusoidal speed fluctuations with $A = 0.0311$, which when substituted in Eqn. (3) yields:

$$\ddot{\alpha}_2 = -0.0311\dot{\alpha}_1^2 \sin(2\dot{\alpha}_1 t) \tag{6}$$

4.1 Time histories

Figure 4 shows the velocity time histories of the oscillating shaft (labelled "stator shaft") and the rotor of the energy harvester (labelled "energy harvester"). These velocities were measured using two-beam laser vibrometers to provide accurate measurements without contacting the device under test. The relative velocity of the energy harvester is calculated by subtracting the energy harvester velocity from the stator

shaft velocity. In Figure 4, the steady state response of the energy harvester is shown at around 1150 rpm mean shaft speed.

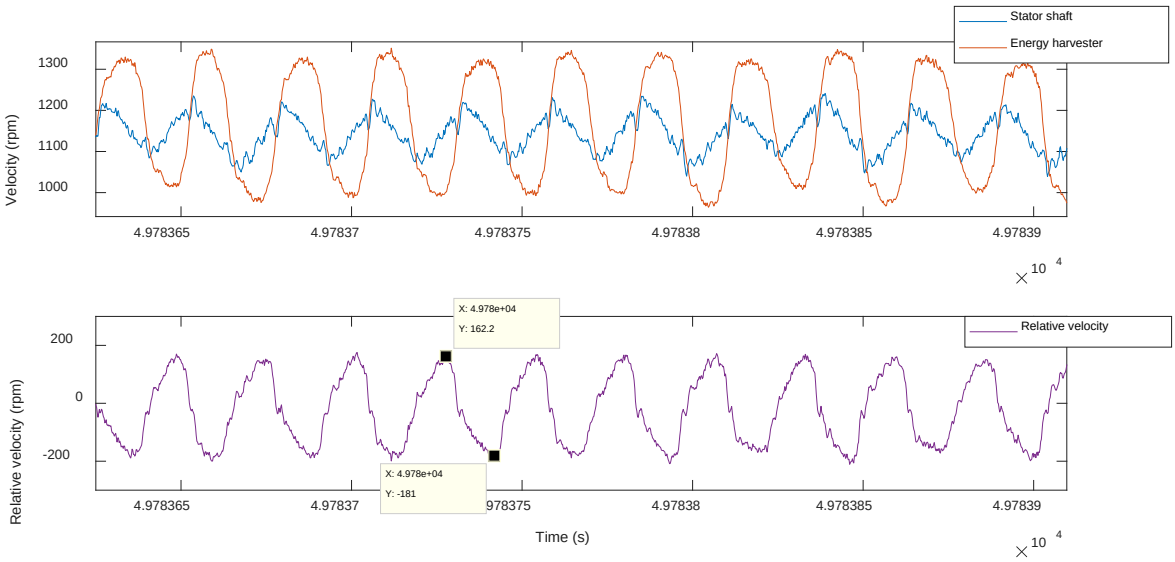

Figure 4: Steady state velocity time histories at 1150 rpm: top – raw shaft speed and energy harvester speed; bottom – relative velocity of the energy harvester.

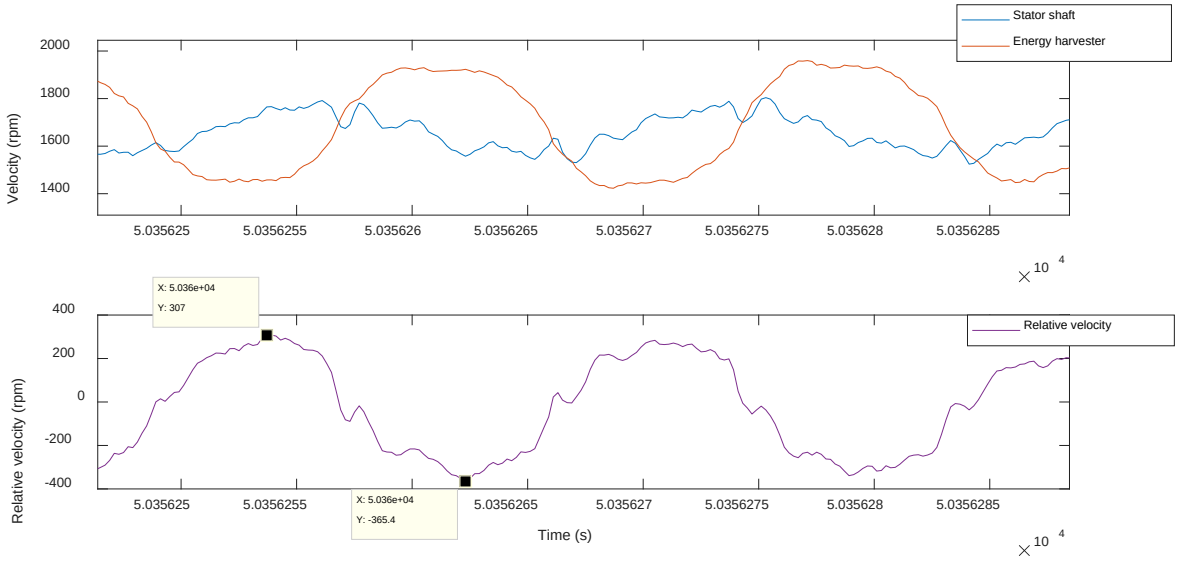

Figure 5: High energy branch solution at 1700 rpm: top – raw shaft speed and energy harvester speed; bottom – relative velocity of the energy harvester.

Figure 5 shows the higher energy stable branch solution at approximately 1700 rpm mean driving shaft speed. The amplitude of the relative velocity is approximately 336.2 rpm as indicated by the insets of the bottom half of Figure 5. The lower stable branch solution at 1700 rpm mean driving speed is depicted in Figure 6. For the same driving conditions as in Figure 5, much lower response amplitude is observed with a relative velocity of approximately 127 rpm. Furthermore, the energy harvester is 180° out of phase with the shaft velocity in the lower energy branch response compared to about 90° out of phase in the higher energy branch response shown in Figure 5. Thus, it can be clearly seen that two distinct stable solutions exist when the driving shaft operates at 1700 rpm with corresponding speed fluctuations as calculated using Eqn. (3).

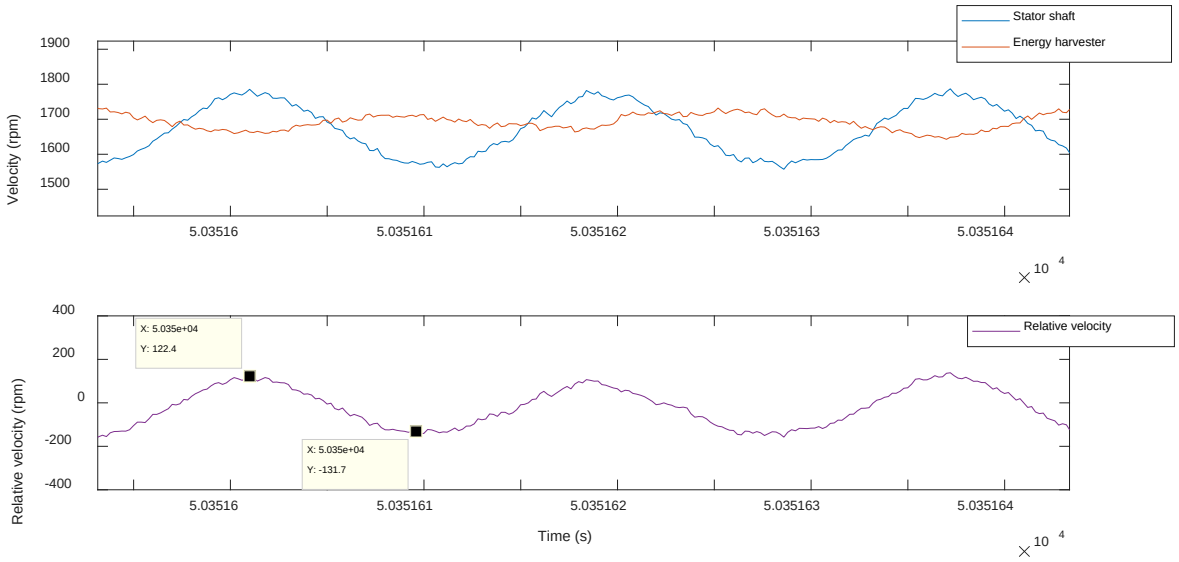

Figure 6: Low energy branch solution at 1700 rpm: top – raw shaft speed and energy harvester speed; bottom – relative velocity of the energy harvester.

4.2 Frequency response diagram

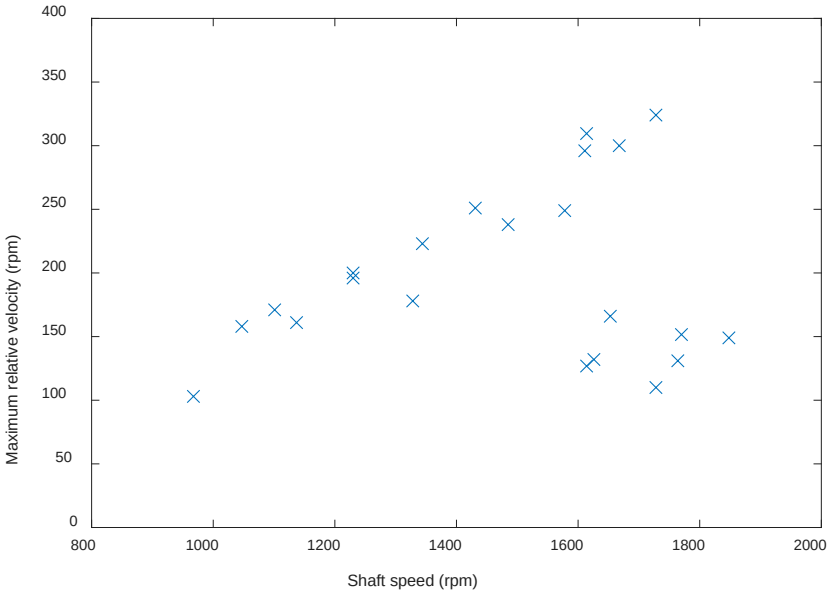

Figure 7: Experimental frequency response graph of the relative velocity

Figure 7 depicts the frequency response graph of the experimental energy harvester. The drive motor was accelerated gradually by manually adjusting the speed control dial of the inverter. At each speed the shaft was allowed to run for at least 30 s to ensure that any transients have faded. From the measured data, the relative velocity was calculated as stated above at each test point. These values are then plotted against the mean shaft speed. Figure 7 follows the same general trend as in Figure 3. At low speeds (<1600rpm in Figure 7, <2800 rpm in Figure 3) there exists only one stable solution. Above this speed threshold, two stable solutions appear. In Figure 7, the high energy branch is maintained until around 1730 rpm however, unlike Figure 3, where the upper stable branch was unattainable above 1730 rpm. This is due to the need for system identification in order to use the right data in the numerical calculations.

5 Conclusions

A physical prototype of a torsional electromagnetic energy harvester has been presented. The experimental results exhibit similar trend as in the predicted model response. A lower energy branch solution region exists at low speeds, followed by a higher energy region, where stable solutions coexist. Further work is required in order to identify the accurate system features and to separate further the upper stable branch from the unstable solution in order to decrease the likelihood of dropping to the lower energy stable branch (and increase the power output potential of the device).

6 References

[1] G. W. Kim, "Piezoelectric energy harvesting from torsional vibration in internal combustion engines," *Int. J. Automot. Technol.*, vol. 16, no. 4, pp. 645–651, Aug. 2015.

[2] A. Z. Trimble, J. H. Lang, J. Pabon, and A. Slocum, "A Device for Harvesting Energy From Rotational Vibrations," *J. Mech. Des.*, vol. 132, no. 9, p. 091001, 2010.

[3] S. Roundy and J. Tola, "Energy harvester for rotating environments using offset pendulum and nonlinear dynamics," *Smart Mater. Struct.*, vol. 23, no. 10, p. 105004, 2014.

[4] L. Gu and C. Livermore, "Passive self-tuning energy harvester for extracting energy from rotational motion," *Appl. Phys. Lett.*, vol. 97, no. 8, 2010.

[5] L. Gu and C. Livermore, "Compact passively self-tuning energy harvesting for rotating applications," *Smart Mater. Struct.*, vol. 21, no. 1, p. 015002, 2012.

[6] B. P. Mann and N. D. Sims, "Energy harvesting from the nonlinear oscillations of magnetic levitation," *J. Sound Vib.*, vol. 319, no. 1–2, pp. 515–530, 2009.

[7] L. Liu and F. G. Yuan, "Nonlinear vibration energy harvester using diamagnetic levitation," *Appl. Phys. Lett.*, vol. 98, no. 20, pp. 2009–2012, 2011.

[8] F. Schmelz, C. H.-C. Seherr-Thoss, and E. Aucktor, *Universal Joints and Driveshafts*, English Ed. Berlin: Springer-Verlag, 1992.

[9] B. Gunn, S. Theodossiades, S. Rothberg, and T. Saunders, "An electromagnetic energy harvester for rotational applications," *Proc. ASME Des. Eng. Tech. Conf.*, vol. 8, 2017.

[10] M. Markovic and Y. Perriard, "An analytical formula for the back emf of a slotted BLDC motor," *Proc. IEEE Int. Electr. Mach. Drives Conf. IEMDC 2007*, vol. 2, pp. 1534–1539, 2007.

[11] E. J. . Doedel, T. F. . Fairgrieve, B. Sandstede, A. R. . Champneys, Y. A. ; Kuznetsov, and X. Wang, "AUTO-07P: Continuation and bifurcation software for ordinary differential equations (2007)." 2007.